Available online at www.sciencedirect.com
SCIENCE DIRECT
Medical Engineering & Physics 28 (2006) 6–12
Medical Engineering & Physics
www.elsevier.com/locate/medengphy

The role of the arterial prestress in blood flow dynamics

Giuseppe Pontrelli*

Istituto per le Applicazioni del Calcolo - CNR, Viale del Policlinico, 137-00161 Rome, Italy

Received 2 November 2004; accepted 11 April 2005

Abstract

Blood flowing in a vessel is modelled using one-dimensional equations derived from the Navier–Stokes theory on the base of long pressure wavelength. The vessel wall is modelled as an initially highly prestressed elastic membrane, which slightly deforms under the blood pressure pulses. On the stressed configuration, the vessel wall undergoes, even in larger arteries, small deformation and its motion is linearized around such initial prestressed state.

The mechanical fluid–wall interaction is expressed by a set of four partial differential equations. To account for a global circulation features, the distributed model is coupled with a six compartments lumped parameter model which provide the proper boundary conditions by reproducing the correct waveforms entering into the vessel and avoid unphysical reflections. The solution has been computed numerically: the space derivatives are discretized by a finite difference method on a staggered grid and a Runge–Kutta scheme is used to advance the solution in time. Numerical experiments show the role of the initial stresses in the flow dynamics and the wall deformation.

Keywords: Wall–fluid interaction; Blood flow; Initial prestretch; Arterial prestress; Numerical methods

1. Introduction

The study of the propagation of pulse waves in arteries has attracted many researchers in biomedical engineering. The relevance of theoretical and clinical aspects of such problem is widely recognized in cardiovascular mechanics, angiology and atherogenesis [1].

The complexity of the *blood-wall* system and the different time and space scales involved in vascular flows stimulate the formulation of reduced models, aimed to analyze and solve simpler problems. For wave propagation phenomena, the mechanical model of an inflated elastic tube filled with an incompressible liquid is commonly used. As the pressure wave travels, the tube deforms under the influence of internal elastic forces and external loads. The wave dynamics strictly depends on the interaction between blood flow and arterial wall [2].

For long wavelengths and being the axial dimension prevailing on the others, one-dimensional models are usually proposed and offer quite satisfactory results [3]. They are built by averaging variables over the cross section A of the tube and describe the mean flow dynamics. Several models based on the tube law of type $A = A(p, x)$ have been developed [2,3]. They do not include any wall displacement along the axial direction due to the fluid shear stress: this can be of some importance when remodelling process and growth of the arterial endothelium are considered. A more realistic approach is obtained when the arterial wall is modelled as a two-dimensional anisotropic membrane that deforms under the forces exerted by the fluid in its tangential plane [4]. Moreover, arteries are naturally under longitudinal and circumferential tensions and in vivo measurements point out the presence of longitudinal stretch and stress [5–7]. Some other work has been done on a theoretical base to extend the Womersley solution to an initially stressed elastic tube [8]. Though much smaller than the radial displacement and generally neglected, the longitudinal wall motion needs a deeper study in vascular mechanics, since it is revealed of some importance in the analysis of the wall shear stress and may have interest in the investigation of pathologies.

A mathematical model with such characteristics has been recently developed. The full nonlinear coupled wall-fluid system has been solved numerically and the flow and of the wall

* Tel.: +39 6 8847 0251; fax: +39 6 4404 306.
E-mail address: g.pontrelli@iac.cnr.it (G. Pontrelli).

1350-4533/$ – see front matter © 2005 IPEM. Published by Elsevier Ltd. All rights reserved.
doi:10.1016/j.medengphy.2005.04.013

deformation dependence on the elasticity parameter has been highlighted [9]. The alternative approach proposed here is to apply the theory of infinitesimal elasticity to the small incremental deformations. Because arterial walls undergo only small changes at each cardiac cycle, the degree of local nonlinear behaviour is small and can be locally linearized [10]. On the other hand, the deformations leading from an unstressed state to an initial stressed configuration are very large, and a nonlinear theory has to be used to compute the initial stress [6].

The purpose of this study is to develop a simple one-dimensional model for the fluid-structure problem describing the blood flow and the wave propagation in an arterial segment. The wall constitutive equation for the vascular tissue proposed in [6] has been used to derive both the longitudinal and circumferential prestretches and prestresses (Section 2) and the linearized wall–fluid equations are written over such initial configuration (Section 3). Since numerical simulations should be performed in a tube of finite length, the problem of assigning suitable inflow and outflow conditions is circumvented by using a lumped parameter model [11]. The resulting coupled system form a unique closed-loop and no boundary conditions for the flow is required (*multiscale model*, Section 4). Finally, many computational results show the appropriateness of such an approach, and evidence the role of the prestreches on the fluid-wall mechanics (Section 5).

2. Mathematical formulation

Blood flowing in a compliant tube as an artery is a complex dynamical system and constitutes a genuine fluid-structure problem. The fluid motion and the wall deformation are mutually influenced and their coupling is responsible for effects, which cannot be explained by each of them alone. When wave propagation phenomena are concerned, simplified models for the system "blood–arterial wall" can be devised. In particular, due to the small deformations of the vascular wall and for the unidirectional nature of blood flow, a one-dimensional model is adopted.

2.1. The flow equations

Let us consider a homogeneous fluid of density ρ and viscosity μ, flowing in a straight, axisymmetric, distensible tube of circular cross section. A cylindrical coordinate system with x as symmetry axis is used. The quasi-1D cross averaged momentum equation are [2]:

$$\frac{\partial u}{\partial t} + u\frac{\partial u}{\partial x} = -\frac{1}{\rho}\frac{\partial p}{\partial x} + f \tag{2.1}$$

where u is the axial velocity, p the transmural pressure, both averaged over the cross section, and t denotes the time. The viscous term f is approximated by the friction term of the Poiseuille steady flow in a tube of radius R:

$$f \simeq -\frac{8\mu u}{\rho R^2} \tag{2.2}$$

As a consequence, the wall shear stress is given by

$$\tau = \mu \left.\frac{\mathrm{d}u}{\mathrm{d}r}\right|_{r=R} = \frac{4\mu u}{R} \tag{2.3}$$

Strictly speaking, the expressions (2.2) and (2.3) hold for a steady flow in a rigid tube, but they are considered acceptable for quasi steady flows and for small deformations [3].

The principle of conservation of mass in a deformable tube is expressed by the following continuity equation [2]:

$$\frac{\partial R}{\partial t} + \frac{R}{2}\frac{\partial u}{\partial x} + u\frac{\partial R}{\partial x} = 0 \tag{2.4}$$

2.2. The wall equations

The vessel wall is modelled as an elastic axisymmetric membrane, that is a 2D thin shell with a mass negligible (wall thickness $\to 0$) compared with that of the fluid contained in it. The membrane, which has no bending stiffness, is capable to deform under the forces exerted by the fluid (i.e. the shear stress τ and the transmural pressure p - cfr. (2.3)). Let $(x_P(s), r_P(s))$ be the Lagrangian coordinates of a particle P with s a parametric coordinate along the membrane in its symmetry plane. In such reference frame, the principal deformation ratios in the axial and circumferential directions are respectively:

$$\lambda_1 = \sqrt{\left(\frac{\mathrm{d}r_P}{\mathrm{d}s}\right)^2 + \left(\frac{\mathrm{d}x_P}{\mathrm{d}s}\right)^2}, \qquad \lambda_2 = \frac{r_P}{R^0} \tag{2.5}$$

where R^0 is the undeformed radius (corresponding to the zero transmural pressure – see Section 3).

Since the fluid equations are expressed in Eulerian coordinates, let us make a change of variables and let $R(x, t)$ and $S(x, t)$ be the Eulerian counterparts of the Lagrangian coordinates of a particle of the a membrane. In such coordinate system, the stretches (2.5) are written as

$$\lambda_1 = \sqrt{\frac{1 + R'^2}{S'^2}}, \qquad \lambda_2 = \frac{R}{R^0} \tag{2.6}$$

(the prime denotes x-derivative). By balance of forces, the fluid–membrane equilibrium equations in tangential and normal directions are provided [4]:

$$\begin{aligned} &R'(T_1 - T_2) + RT_1' = \rho\tau R(1 + R'^2)^{1/2}, \\ &\frac{-R''}{(1 + R'^2)^{3/2}}T_1 + \frac{1}{R(1 + R'^2)^{1/2}}T_2 = p \end{aligned} \tag{2.7}$$

where T_1 and T_2 are the longitudinal and circumferential stresses, respectively. Let us now define a constitutive equation for the arterial vessel that give an expression for T_1 and T_2 in Eq. (2.7). For an incompressible hyperelastic material,

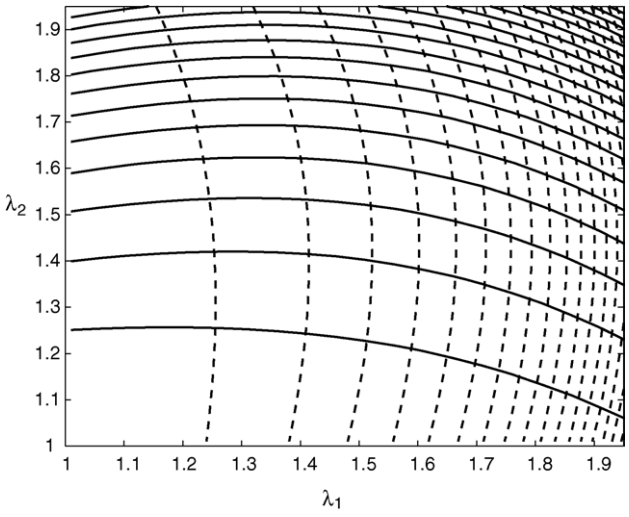

Fig. 1. Contour plot of the stresses T_1 (dashed line) and T_2 (solid line), as in Eqs. (2.9) and (2.10), with $c_1 = 0.38$, $c_2 = 0.26$, $c_3 = 0.046$.

it is possible to define a strain-energy function W as a function of the principal strains: it represents the elastically stored energy per unit volume in terms of the strain variables and is a potential for the stress [7].

Based on a series of experiments on canine arterial specimens, a strain-energy density function w modelling the mechanical properties of the arterial wall has been recently proposed by Zhou and Fung [6] as

$$w = c\,(\exp(Q) - 1), \qquad Q = c_1 E_1^2 + c_2 E_2^2 + 2c_3 E_1 E_2 \tag{2.8}$$

where c is a material parameter having the dimensions of $dyne/cm$, c_1, c_2, c_3 are nondimensional constants (with $c_1 \approx c_2$ and $c_1, c_2 \gg c_3$) and $E_k = \frac{1}{2}(\lambda_k^2 - 1) \quad k = 1, 2$ are the principal Green strains. Hence, the stress components (averaged across the thickness) along the longitudinal and circumferential directions are given by differentiation of w:

$$T_1(\lambda_1, \lambda_2) = \frac{\lambda_1}{\lambda_2}\frac{\partial w}{\partial E_1} = \frac{1}{\lambda_2}\frac{\partial w}{\partial \lambda_1} = 2\frac{\lambda_1}{\lambda_2}\,c\,(c_1 E_1 + c_3 E_2)\exp(Q) \tag{2.9}$$

$$T_2(\lambda_1, \lambda_2) = \frac{\lambda_2}{\lambda_1}\frac{\partial w}{\partial E_2} = \frac{1}{\lambda_1}\frac{\partial w}{\partial \lambda_2} = 2\frac{\lambda_2}{\lambda_1}\,c\,(c_3 E_1 + c_2 E_2)\exp(Q) \tag{2.10}$$

The former relations hold in the case of an incompressible and anisotropic material, wherein principal directions of strain and stress coincide and express the property that the instantaneous Young's modulus increases with the strain, but with a different amount in the two directions (Fig. 1). The full nonlinear fluid-wall interaction problem has been solved in [9].

3. Linearization of the wall dynamics equations

Despite the nonlinear character of the strain–stress Eqs. (2.9) and (2.10), the wall deformation, even in large arteries, can be regarded as the resultant of a large nonlinear deformation and a small superimposed linear fluctuations over it (see Fig. 2). This suggests to linearize the wall equilibrium Eq. (2.7) as follows. All the dependent variables are expanded in power series of a small parameter ε as $\chi = \chi^* + \varepsilon\tilde{\chi} + \varepsilon^2\tilde{\chi}_2 + \cdots$ and substituted in the governing equations. In the linearization process, all the terms

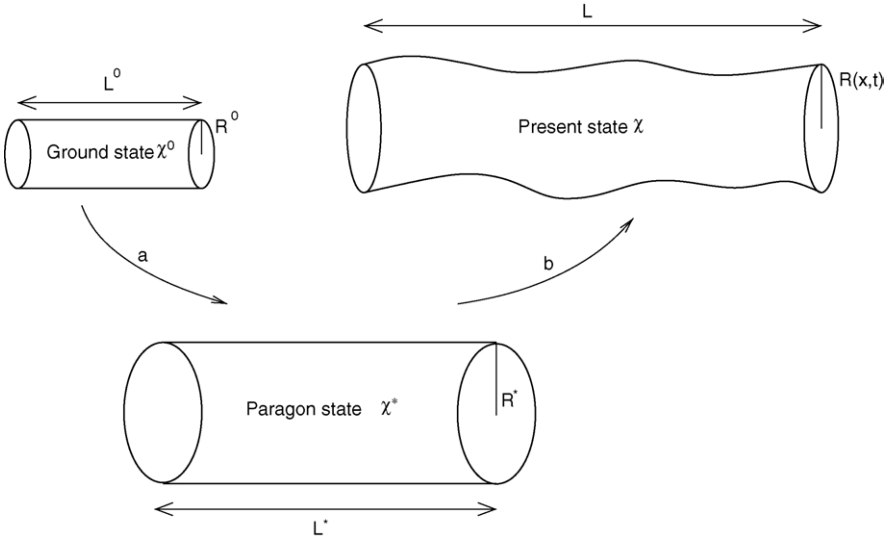

Fig. 2. Schematic decomposition of the motion in a nonlinear large deformation (a) and a small linear deformation (b). The present configuration χ is regarded as a small variation on the paragon state χ^*.

containing powers of ε of order greater than one are higher order infinitesimals and have been neglected. The state χ^*, corresponding to $\varepsilon = 0$, is the 0th order approximation and can be considered as a known initial (stressed) state of the motion and the present state χ is regarded as a first-order perturbed state (of magnitude $\varepsilon\tilde{\chi}$) over χ^*. We therefore assume that the excess stresses are related to the correspondent excess strains linearly.

From a mechanical point of view, an ideal stress-free configuration χ^0 (or *natural* or *ground* state) is defined as the possible state where no forces act on the wall ($p^0 = 0$). It is characterized by a constant radius R^0 and finite length L^0. We then define a reference (or *paragon*) stressed steady configuration χ^* as the state of an inflated (with a constant load p^*) and uniformly stretched tube (of finite length L^*). Such a state is defined by a solution of Eq. (2.7), having $R^* = const.$ and $S^*(x) = x$ (see [10]). The longitudinal and the circumferential stretches in the paragon configuration, referred to the ground state, are defined as

$$\lambda_1^* = \frac{L^*}{L^0}, \qquad \lambda_2^* = \frac{R^*}{R^0} \tag{3.1}$$

By using Eqs. (2.9) and (2.10) the stresses in paragon configuration are constant and given by

$$T_1^*(\lambda_1^*, \lambda_2^*) = 2\,c\,\frac{\lambda_1^*}{\lambda_2^*}(c_1E_1^* + c_3E_2^*)\exp(Q^*),$$

$$T_2^*(\lambda_1^*, \lambda_2^*) = 2\,c\,\frac{\lambda_2^*}{\lambda_1^*}(c_3E_1^* + c_2E_2^*)\exp(Q^*) \tag{3.2}$$

with $Q^* = Q(\lambda_1^*, \lambda_2^*)$ and $E_k^* = E_k(\lambda_k^*)$.

The stretches λ_1^*, λ_2^* and the stresses T_1^*, T_2^* are related through Eq. (3.2) and are sometimes referred to as *prestretches* and *prestresses*. They are the initial reference parameters and the ones or the others are assumed preassigned. From Eq. (2.7), it follows that

$$T_2^* = p^* R^* \quad \textit{Laplace's law} \tag{3.3}$$

We now linearize the stretches and the stresses around the paragon state χ^*. Hence, for $\tilde{R}$ and $\tilde{S}'$ small, the longitudinal and hoop stretches at the present configuration are given by

$$\lambda_1 = (1 + \tilde{S}')\lambda_1^*, \qquad \lambda_2 = \left(1 + \frac{\tilde{R}}{R^*}\right)\lambda_2^* \tag{3.4}$$

Accordingly, the linearized constitutive laws relating the stresses T_1 and T_2 to $\tilde{S}'$ and $\tilde{R}$ are

$$T_1 = (T_1^* + D_{11}^*)\,\tilde{S}' + (-T_1^* + D_{12}^*)\,\frac{\tilde{R}}{R^*},$$

$$T_2 = (-T_2^* + D_{21}^*)\,\tilde{S}' + (T_2^* + D_{22}^*)\frac{\tilde{R}}{R^*} \tag{3.5}$$

obtained by a linearization of (2.9) and (2.10) around the paragon configuration, where

$$D_{11}^* = c\frac{(\lambda_1^*)^3}{\lambda_2^*}[c_1 + 2(c_1E_1^* + c_3E_2^*)^2]\exp(Q^*),$$

$$D_{22}^* = c\frac{(\lambda_2^*)^3}{\lambda_1^*}[c_2 + 2(c_3E_1^* + c_2E_2^*)^2]\exp(Q^*),$$

$$D_{12}^* = D_{21}^* = c\lambda_1^*\lambda_2^*[c_3 + 2(c_1E_1^* + c_3E_2^*) \times (c_3E_1^* + c_2E_2^*)]\exp(Q^*) \tag{3.6}$$

It is worth noting that the constitutive laws (3.5) depend nonlinearly on the prestretches λ_1^* and λ_2^* but linearly on $\tilde{R}$ and on $\tilde{S}'$; moreover, if $\lambda_1^* = \lambda_2^* = 1$ (i.e. the paragon configuration is the ground state) they reduce to the standard linear strain–stresses constitutive relations of an anisotropic membrane.

By using (3.5), the wall motion Eq. (2.7) are therefore linearized around the paragon state χ^* as

$$(T_1^* + D_{11}^*)\tilde{S}'' + (-T_2^* + D_{12}^*)\frac{\tilde{R}'}{R^*} = \rho\tau,$$

$$-T_1^*\,\tilde{R}'' + \frac{1}{R^*}(-T_2^* + D_{21}^*)\tilde{S}' + D_{22}^*\frac{\tilde{R}}{(R^*)^2} = \tilde{p} \tag{3.7}$$

where $\tilde{p}$ is the excess pressure ($p = p^* + \varepsilon\tilde{p}$).

The fluid nonlinearity has an intrinsic significance, being the inertial effect dominant in large vessels, and cannot be eliminated. For uniformity of notation, Eqs. (2.1) and (2.4) are rewritten with respect to the paragon configuration respectively as

$$\frac{\partial\tilde{u}}{\partial t} + (u^* + \tilde{u})\frac{\partial\tilde{u}}{\partial x} = -\frac{1}{\rho}\frac{\partial\tilde{p}}{\partial x} + f \tag{3.8}$$

$$\frac{\partial\tilde{R}}{\partial t} + \frac{R^* + \tilde{R}}{2}\frac{\partial\tilde{u}}{\partial x} + (u^* + \tilde{u})\frac{\partial\tilde{R}}{\partial x} = 0 \tag{3.9}$$

with u^* a constant velocity satisfying the flow and the continuity equations at the paragon state (for a viscous flow, $u^* = 0$).

4. Boundary conditions and multiscale models

The linearized wall Eq. (3.7) and the fluid flow Eqs. (3.8) and (3.9) have to be solved in a finite domain representing an arterial segment. Such a segment is extracted from the arterial tree and boundary conditions of physical significance for the variables are required. When balance of flows and pressures for the systemic circulation has to be taken into account, models for the closed-loop system should be addressed. They are built by partitioning the whole vascular tree in elementary districts and by "lumping" the dynamical variables in each of them (lumped parameter or 0D models). These models date back to the pioneeristic works of Westerhof et al. and are based on the analogy between hydraulic networks and electrical circuits [12]. In each compartment the values of the resistance, compliance and inertial parameters are constant and a linear differential

relationship between flow and pressure is given. These elementary blocks are linked between them and connected with the *heart* pump to form a closed loop representing the cardiovascular system. The whole model describes the time evolution of the mean values of the variables in each section.

To account for a comprehensive system of the global circulation, the six compartment lumped model described by Avanzolini et al. [13] is used. Following [11], we have inserted the distributed wall–fluid model in the point of network corresponding to the descending aorta (Fig. 3). This approach (*multiscale model*) allows to implicitly assign boundary conditions for the distributed system. These are easily expressed as a functions of lumped variables to guarantee the continuity of flow and pressure at the interfaces.

The coupled system is equivalent to a 1D model for the full circulatory system where, except for a segment, the remaining arterial tree has been truncated and lumped in a finite number of blocks. On the other way around, the coupled model can be regarded as a lumped parameter model where a compartment has been expanded in a distributed model.

If the coupling strategy eliminates the drawback of assigning a boundary value for u and p, wall displacement conditions at the extrema of the vessel are to be provided. These are given by considering a *long* vessel (i.e. of length much larger than the reference radius R^*) with free ends. Therefore, the conditions:

$$R' = R'' = 0, \quad S' = 1 \tag{4.1}$$

hold at the ends. This implies that

$$\tilde{R}' = \tilde{R}'' = 0, \quad \tilde{S}' = \tilde{S}'' = 0 \tag{4.2}$$

From (3.7.2) it follows that the implicit relation between $\tilde{R}$ and $\tilde{p}$:

$$D_{22}^* \tilde{R} = \tilde{p}\,(R^*)^2 \tag{4.3}$$

holds at both ends. Such a condition unifies the four conditions (4.2). Moreover, the boundary conditions on S:

$$S(0,t) = 0, \qquad S(L,t) = \bar{L}$$

expressing a finite axial deformation are imposed. This implies that:

$$\tilde{S}(0,t) = 0, \quad \tilde{S}(L,t) = \bar{L} - L^* \tag{4.4}$$

For details on the implementation of the multiscale algorithm and on the procedure of coupling models of different physical dimension, see [9].

5. Results and discussion

To solve the 1D fluid–structure model numerically, Eqs. (3.7)–(3.9) are solved simultaneously in a finite interval $[0, \mathcal{L}]$. Let us consider a sequence of $n+1$ equispaced grid points $(x_i)_{i=0,\dots,n}$ with $x_0 = 0$ and $x_n = \mathcal{L}$. The spatial discretization is obtained by evaluating membrane prestretches and prestresses (see Eqs. (3.1), (3.2), (3.6)) at n inner points $\xi_i = (x_i + x_i + 1)/2$ of a staggered grid by considering averaged neighboring variables. On the other hand, wall–fluid equilibrium Eq. (3.7) and flow Eqs. (3.8) and (3.9) are computed at the $n-1$ inner points x_i. In the following numerical experiments, the spatial mesh has been obtained by dividing the length of the vessel $L = 8$ cm in 800 equal parts ($\Delta x = 0.01$ cm) and with a time step $\Delta t = 10^{-4}$ s. The 1D model is inserted in correspondence of the descending aortic artery (Fig. 3) and is solved coupled with the 0D model. The Runge–Kutta scheme of second order has been used both in the distributed and the lumped parameter model to advance in time. The choice of the above numerical parameters guarantees stability and grid independence. The resulting nonlinear algebraic system is solved by a globally convergent Newton type method.

The following numerical values for the distributed model are used:

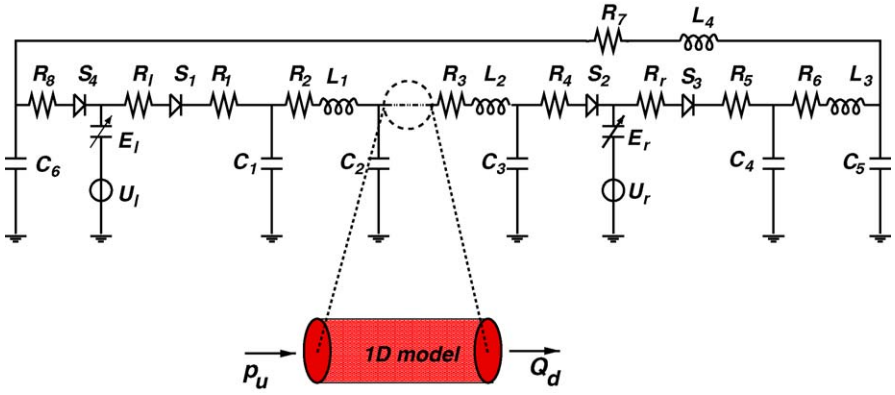

Fig. 3. Coupling of 0D and 1D models at the level of the descending aorta. Pressure and flow variables are exchanged at the interface points to guarantee continuity (by courtesy of Formaggia et al. [11]).

$$c = 2 \times 10^5\,\text{dyne/cm}, \qquad c_1 = 0.38, \qquad c_2 = 0.26,$$
$$c_3 = 0.046, \quad R^* = 1.2\,\text{cm}, \quad L^* = \bar{L} = 8\,\text{cm},$$
$$\rho = 1.05\,\text{g/cm}^3$$

(note that c in (2.8) is obtained by integration across the wall thickness of the analogous density energy function in Zhou and Fung [6] and the other material constants are determined from *in vivo* experimental data [6]).

In a large vessel, as that considered here, the frictional force due to the fluid viscosity is comparatively small and is disregarded. Actually, experiments carried out with and without the fluid viscosity do not exhibit remarkable quantitative differences. For the lumped parameter model the same parameters R_k, C_k, L_k as in [13] have been used. In all the simulations, the dependence of the small motions on the prestretches $(\lambda_1^*, \lambda_2^*)$ is investigated. Subject to the heart pressure, transmitted through the 0D model, the wall expands up to a mean value of R and oscillates periodically between a maximum and a minimum limits. Similarly, all the flow variables have a periodical small fluctuations over a mean value. In particular, the values of R and S depend not only on the elasticity coefficient c, but on the reference radius R^*.

The behaviour of the variables R and S in the mid point are depicted for three values of the initial stretch λ_2^* (with λ_1^* fixed) in Fig. 4, and for varied λ_1^* (with λ_2^* unchanged) in Fig. 5, and evidence a different mechanical response in the two directions. The radial displacement R decreases monotonically with λ_2^*. Furthermore, the variation of R on the prestretch λ_2^* is much larger than the variation on λ_1^*. On the other hand, it first increases and then decreases with the axial prestretch: a maximum is attained at about $\lambda_1^* = 1.4$ for all circumferential prestretches (this behaviour is related to the material properties along the two directions (cfr. Eqs. (2.9), (2.10), and see Fig. 6).

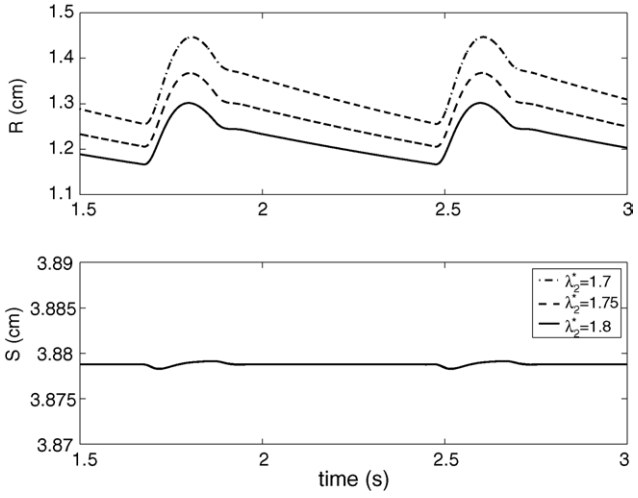

Fig. 4. Time histories for R, S at the center of the artery for three values of the circumferential prestress λ_2^* ($\lambda_1^* = 1.4$). Longitudinal deformation S is small (cfr. the different scale) and almost insensitive to λ_2^*.

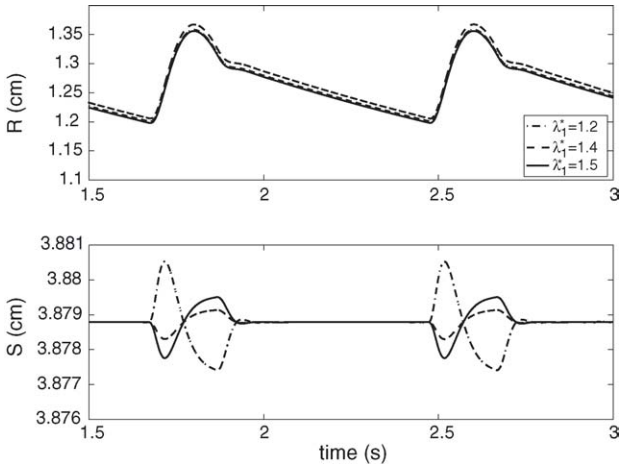

Fig. 5. Time histories for R, S at the center of the artery for three values of the longitudinal prestress λ_1^* ($\lambda_2^* = 1.75$). Longitudinal deformation S is small (cfr the different scale), but its variation are quite effective with λ_1^* in correspondance to the pressure peak.

The variation of the longitudinal displacement S is comparatively smaller, but is more sensitive to the variation of λ_1^*. Marked changes of S occur in correspondence of large variation of the pressure, and of its derivatives (Fig. 5). The fluid dynamical variables p and u are less sensitive to the initial state of stress.

The solution has been found for a limited range of the prestretches: these probably correspond to the admissible values of the elastic energy function (2.8). Actually, the values of R^*, p^* and c (as well as of λ_1^*, λ_2^*) cannot be chosen independently, but should satisfy a compatibility condition (see Eqs. (3.1)–(3.3)). Another restriction comes from the presence of the lumped parameter model which, coupled to the distributed model, should provide consistent values of the pressure and flows (see Section 4). In particular the global pressure should be compatible with the initial stretch and

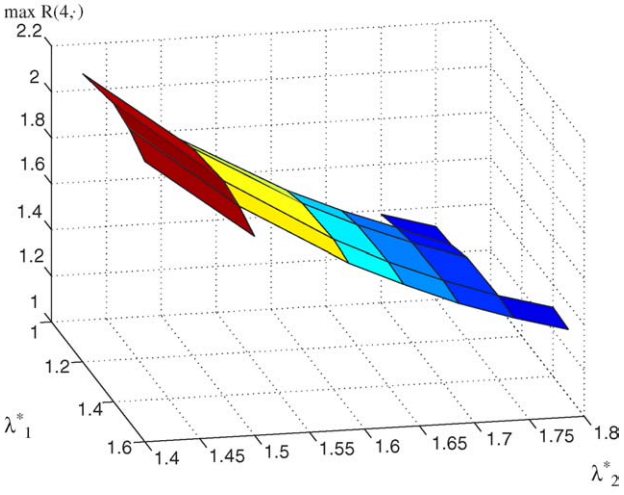

Fig. 6. Maximum radial deformation for varying prestretches. The surface is obtained by a linear fit of simulated values and shows as different mechanical behaviour in the two directions.

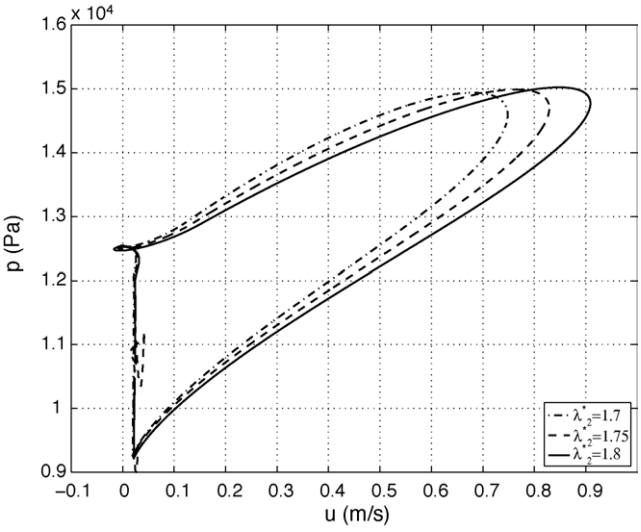

Fig. 7. PU loop curves in the central point of the vessel. Slopes of such curves indicate the local wave speed when no reflections are present. The plot evidences the influence of the circumferential prestress λ_2^* (with $\lambda_1^* = 1.4$ fixed) on the mean fluid velocity, on the pressure and on the wave speed.

tension according to Eq. (3.3). For large λ_2^* the wall stiffens and undergoes a smaller deformation. Over a critical value, the radial deformation, at some instants, is below the reference radius R^*. In such a case the mean pressure is below the reference pressure $p^* = T_2^*/R^*$ and a moderate buckling takes place (the prestretch is not compatible with the inflow pressure). On the other way around, for a low value of λ_2^*, the vessel wall undergoes large deformations that cannot be adequately represented by the present 1D linearized model.

In a recent work, the same problem has been studied by solving the full nonlinear equations for the wall over an unstressed reference state (see Eqs. (2.7), (2.9), (2.10)) [9]. A comparison with the simulation in [9] having the same numerical parameters show that similar results are obtained in correspondence of $\lambda_1^* = 1.4$ and $\lambda_2^* = 1.8$ and demonstrate the adequacy of the linearization.

In principle, the velocity of the wave can be obtained by fixing two points in the vessel and measuring the crossing time of a peak. However, such a procedure is not accurate over a short length and for the time and space steps as those considered in this work. Moreover the profiles change their shape as they travel, and it is difficult to follow a profile in time [8]. As a consequence, the computed speed value measured for u, p and R between the same grid points may be different, and varies in time.

Khir and Parkers [14] suggest another method to measure the wave speed γ in elastic tubes in absence of reflected waves. It is based on the validity of the water–hammer equation $\mathrm{d}p = \pm\rho\gamma\,\mathrm{d}u$ and consists in measuring the slope of the PU loop curves. For a typical PU loop as that displayed in Fig. 7, the local wave speed is $\gamma = 5.2$ m/s ($\lambda_1^* = 1.4$, $\lambda_2^* = 1.8$, solid line), in agreement with experiments. Following such method, it is shown that initial hoop stretching hinders the propagation of the pulses, while no significant differences are related to axial loading.

Acknowledgments

The author would like to thank Paola Nardinocchi and Luciano Teresi for their useful suggestions and criticism during this work.

References

[1] O' Rourke MF. Vascular mechanics in the clinic. J Biomech 2003;36:623–30.
[2] Fung YC. Biomechanics: circulation. 2nd ed. New York: Springer-Verlag; 1997.
[3] Reuderink PJ, Hoogstraten HW, Siupkema P, Hillen B, Westerhof N. Linear and nonlinear one-dimensional model of pulse wave transmission at high Womersley numbers. J Biomech 1989;22(8/9):819–27.
[4] Pedrizzetti G. Fluid flow in a tube with an elastic membrane insertion. J Fluid Mech 1998;375:39–64.
[5] Kuiken GDC. Wave propagation in a thin-walled liquid-filled initially stressed tube. J Fluid Mech 1984;141:289–308.
[6] Zhou J, Fung YC. The degree of nonlinearity and anisotropy of blood vessel elasticity. Proc Natl Acad Sci USA 1997;94:14255–60.
[7] Schulze-Bauer CHJ, Holzapfel GA. Determination of constitutive equations for human arteries from clinical data. J Biomech 2003;36(2):165–9.
[8] Atabek HB, Lew HS. Wave propagation through a viscous incompressible fluid contained in an initially stressed elastic tube. Biophys J 1966;6:481–503.
[9] Pontrelli G. A multiscale approach for modelling wave propagation in an arterial segment. Comp Meth Biomech Biomed Eng 2004;7:79–89.
[10] Nardinocchi P, Pontrelli G, Teresi L. A one-dimensional model for blood flow in prestressed vessels. Eur J Mech A: Solids 2005;24:23–33.
[11] Formaggia L, Nobile F, Quarteroni A, Veneziani A. Multiscale modelling of the circulatory system: a preliminary analysis. Comput Visual Sci 1999;2:75–83.
[12] Westerhof N, Bosman F, Vries CD, Noordergraaf A. Analog studies of the human systemic arterial tree. J Biomech 1969;2:121–43.
[13] Avanzolini G, Barbini P, Cappello A, Cevenini G. CADCS simulation of the closed-loop cardiovascular system. Int J Biomed Comput 1988;22:39–49.
[14] Khir AW, Parker KH. Measurements of wave speed and reflected waves in elastic tubes and bifurcations. J Biomech 2002;35:775–83.